Biomaterials 31 (2010) 2335–2347

Contents lists available at ScienceDirect

Biomaterials

journal homepage: www.elsevier.com/locate/biomaterials

Cyclodextrin-based device coatings for affinity-based release of antibiotics

Thimma R. Thatiparti, Andrew J. Shoffstall, Horst A. von Recum*

Department of Biomedical Engineering, Case Western Reserve University, 10900 Euclid Ave., Wickenden Room 220, Cleveland, OH 44106, USA

ARTICLE INFO

Article history:
Received 2 October 2009
Accepted 24 November 2009
Available online 21 December 2009

Keywords:
Hydrogel
Polysaccharide
Drug delivery
Controlled release
Affinity
Antibiotic

ABSTRACT

Cyclodextrin-based hydrogels were synthesized to create robust networks with tunable mechanical properties capable of serving as device coatings. The CD networks were able to swell and load drug in aqueous and organic solvents. The rheological properties of the swollen gels were investigated using stress and frequency sweeps, with both demonstrating high storage modulus, indicating strong elastic gels. The ability of the gels to swell in numerous solvents allowed for the separate loading and release of different antibiotic drug molecules with varying hydrophilicities. Based on FTIR and TGA studies, each drug was found to form an inclusion complex with CD. For comparison, dextran gels were prepared similarly. As expected for affinity-based mechanisms, the release of drugs from the CD-based gels was slower than diffusion-based release from the dextran gels, and could be sustained for more than 200 h. Coating potential was tested by coating two different medical devices: metal screws and polymer meshes. The meshes were characterized by SEM, revealing that CD-based coatings resulted in a uniform thin film, whereas the dextran gels only partly coated the device and showed delamination. Considerably longer bactericidal activity against *Staphylococcus aureus* was observed for both the CD hydrogels and coatings, as compared to dextran-based ones. The slow, sustained, affinity-based release of antibiotics from the CD-based networks reflects their potential as a delivery platform.

1. Introduction

Hydrogels have played an important role in the biomedical field for many years due to their hydrophilic nature and potential for developing efficient and safe (biocompatible) drug delivery systems [1,2]. Nevertheless, they have some limitations such as a minimal loading capacity of hydrophobic drugs and typically a rapid, non-linear release by diffusion [3]. Consequently, the development of networks that swell in both aqueous and organic solvents would be beneficial for loading both water and organic solvent soluble drugs. Recently, cyclodextrin (CD)-based hydrogels have become popular due to favorable swelling properties and the ability to form inclusion complexes [4–8]. In this function, the CDs serve as receptors, which can selectively and strongly bind various target molecules. This unique behavior leads CDs to have widespread applications that are useful in chemical, biochemical, biomedical, and pharmaceutical industries as well as other advanced sciences [9]. However, CD-based polymers having these properties are typically synthesized at higher temperatures, which may limit their application to temperature sensitive guest molecules or application to biomedical devices and often leads to undesirable side reactions.

Historically, many attempts have been made to load antibiotics onto medical devices to prevent infections. Typically, these studies have achieved relatively short drug release periods on the order of hours to days. In response, extensive effort has been put into the development of cyclodextrin polymer coatings to further improve drug loading and sustained delivery from medical devices [10–15]. However, the process that has been previously demonstrated to physically coat the device with CD is very tedious and requires harsh conditions such as high temperatures and the use of a catalyst, leading to uncontrolled crosslinking density and a rough coating surface. Additionally, these approaches are often specific to a material or chemistry and not broadly applicable to many different biomedical devices.

We, and others, have previously shown an affinity-based drug delivery platform synthesized using different isocyanate crosslinkers [8,16]. While these polymers showed improved drug release profiles when compared to chemically similar diffusion-only systems, the gelation of these materials required longer than desired heating times and high temperatures. Additionally this process led to the formation of rigid networks possessing low water swelling ($\approx$1.5 g/g) and drug loading capacity (<3%). The work presented herein demonstrates a substantial improvement upon our previous design by both decreasing the gelation temperature

* Corresponding author. Tel.: +1 216 368 5513; fax: +1 216 368 4969.
E-mail address: horst.vonrecum@case.edu (H.A. von Recum).

0142-9612/$ – see front matter © 2009 Elsevier Ltd. All rights reserved.
doi:10.1016/j.biomaterials.2009.11.087

and increasing the swelling capability of the cured networks. This results in a platform which is well suited for device coating applications, since the materials have improved mechanical properties and increased drug loading capacity. In addition, to the best of our knowledge, this is the first report of CD network polymers synthesized at room temperature and in biocompatible solvents, a critical feature for device coating applications, particularly for sensitive devices such as hernia repair meshes or sutures.

To evaluate the capacity of these materials as a broad platform we explored their ability to deliver antibiotics for device-related infection by coating onto both prosthetic meshes and metal screws. The mesh used in this study, Parietex™, is a conventional polyester mesh available in several architectures. In this case, a 3D weave (TET) was used. Ventral hernia repair, one of the most common surgeries performed, is still plagued with device-related infections, occurring up to 30% of the time depending on technique and case complexity [17,18]. Dualmesh® Plus, a commercially available antimicrobial mesh was designed to meet this demand. However therapeutic applicability does not extend beyond 14 days, and these materials have been shown to elicit undesirable activation of the immune system [19]. As such, clinical adoption of these materials has been limited, and there remains no hernia repair material with long-term antibiotic properties.

Similarly, orthopedic implants are plagued by device infection, and there has been extensive investigations in this area, however a device coating which resists infection and bacterial colonization while maintaining good fracture fixation (integration, mechanical strength, etc.) is still elusive [20–24].

2. Experimental

2.1. Materials

β-cyclodextrin polymer (CD, 2–15 kDa, average 10 CDs per chain) was purchased from CTD, Inc. (High Springs, FL); dextran (Dex, 15–20 kDa) was obtained from Polysciences, Inc. (Warrington, PA). Both were dried under vacuum at 100 °C for 24 h and stored in a desiccator before use. 2-Isocyanatoethyl 2,6-diisocyanatohexanoate (LTI, Kyowa Hakko Kogyo, Co. Ltd, Tokyo, Japan) and 1,6-diisocyanatohexane (HDI, Aldrich, St. Louis, MO) were used as received. Rifampin (RM) was purchased from Fisher Scientific. Novobiocin sodium salt (NB) and Vancomycin hydrochloride (VM) were purchased from MP Biomedicals, Inc. (Solon, OH). Polyester mesh (Parietex™ TET) (Covidien, Mansfield, MA) was graciously provided by Dr. Michael Rosen, University Hospitals, Cleveland, OH. Metal orthopedic screws (1.6 mm Kirschner wires, stainless steel threaded) (Zimmer, Warsaw IN) were graciously provided by Dr. Christopher Hernandez, Case Western Reserve University, Cleveland, OH. N, N-Dimethylformamide (DMF) and Dimethylsulfoxide (DMSO) were obtained from Applied Biosystems (Foster City, CA) and were dried over calcium hydride and distilled in high vacuum. All other reagents were purchased from Fisher Scientific and used as received.

2.2. Cyclodextrin network preparation

The low molecular weight β-cyclodextrin polymer (CD) was soluble in water as well as in DMF solvent. Previously, this macromonomer was crosslinked at higher temperature (70 °C) into a polymer network in order to make it insoluble for application as a drug delivery platform [8]. Here we optimized gelation to avoid the use of heating. Briefly, a known amount of CD was dissolved in a desired amount of DMF in a 20 mL sample bottle at room temperature. Then varying quantities of crosslinkers (either LTI or HDI) were added into the CD containing bottles. The feed compositions of CD solutions are shown in Table 1. Upon complete dissolution of the reactants, the reaction mixtures were poured into Teflon Petri dishes (Dish Evap PTFE Low 25 mL, Fisher Scientific) and kept in a compact vacuum oven for 48 h to form gels. The crosslinked gels were then used to punch out sample disks of different sizes. Disks 5 mm in diameter were punched from the gel using a 5 mm stainless steel core punch and used for swelling, drug loading, and release studies. For rheological experiments, disks 12 mm in diameter were punched from the gel using a 12 mm stainless steel punch. All disks were incubated in water and then DMF, sequentially, for 24 h each to remove unreacted products, with periodic replacement of water and DMF during that time period used for leaching. The purified disks were dried under vacuum at 50 °C for 48 h and used for all characterization studies. The same procedure, as described above, was used to synthesize dextran gels except the solvent, DMSO, was used instead of DMF. All gels showed gel content to be more than 90%.

2.3. FTIR

FTIR spectra of the dried hydrogel samples before and after drug loading were recorded over the range 600–4000 cm^{-1} in an Excalibur FTS 3000 Fourier-Transform Infrared Spectrophotometer (Bio-Rad, Hercules, CA). Samples were incorporated in a potassium bromide pellet prior to analysis.

2.4. Thermal analysis

Differential scanning calorimetry (DSC) experiments were performed on a TA Instruments Q100 DSC. The samples were heated from 30 °C to 250 °C at a rate of 10 °C/min under nitrogen (40 mL/min gas flow rate). The sample weights were approximately 5 mg each. Thermo-gravimetric analysis (TGA) was performed on a TA Instruments Q500 TGA with a heating rate of 10 °C/min in a nitrogen atmosphere using a flow rate of 40 mL/min.

2.5. Device coating

New, sterile polyester mesh (12 mm diameter punched disks) and metal screws were placed in a Teflon Petri dish. Known amounts of pre-gel solution (dextran or CD), as were used in the network synthesis discussed above, were poured on top of the mesh and screws with the help of a micropipette to achieve a homogeneous coating. The dishes were placed under vacuum for 48 h, after which the devices were removed and washed as described above.

2.6. Scanning electron microscopy (SEM)

The surface morphology of swollen crosslinked gel samples (after lyophilization) and gel-coated meshes in vacuum dried conditions were examined by scanning electron microscopy (SEM). To prepare samples for SEM, all samples were fixed on a brass stub using double-sided tape and then gold coated in vacuum by a sputter coater. The pictures were taken at an excitation voltage of 5 kV using a Hitachi S4500 SEM (Japan).

2.7. Equilibrium water content and polymer volume fraction

The equilibrium water content was determined in the following manner: Dried hydrogel samples consisting of 5 mm diameter disks were weighed. The samples were then swollen in distilled water or DMF for 24 h after which samples were removed and blotted lightly with filter paper to remove excess water or DMF and weighed again (W_1). The disks were then dried at 100 °C for 1 h and the dry weight determined (W_2). Equilibrium swelling was calculated as $(W_1 - W_2)/W_2$. These studies were performed in triplicate ($n = 3$) with the average values reported.

The polymer volume fraction, φ_2, at equilibrium swelling at 25 °C was calculated from [25]:

$$\varphi_2 = \left(\frac{D_0}{D_1}\right)^{\delta} \quad (1)$$

Table 1
Compositions used to prepare gels.

Sample code	Mole ratio of polymer[a] to crosslinker	Weight of dextran (g)	Weight of CD (g)	Amount of LTI (μL)	Amount of HDI (μL)	Amount of DMF (mL)
Dex–LTI(1:0.16)	1:0.16	1.3		320	–	8.658
Dex–LTI(1:0.32)	1:0.32	1.3		640		8.658
CD–LTI(1:0.16)	1:0.16	–	1.3	320	–	8.658
CD–LTI(1:0.32)	1:0.32	–	1.3	640	–	8.658
CD–HDI(1:0.16)	1:0.16		1.3		200	8.658
CD–HDI(1:0.32)	1:0.32	–	1.3		400	8.658

[a] One glucose unit was used (dextran or CD) to calculate the moles.

where D_0 is the diameter of the hydrogel and D_1 is the diameter of the swollen gel in water.

2.8. Rheology and network parameters

Rheological oscillatory measurements were performed using a controlled stress rheometer (TA instruments AR2000(ex) rheometer). The geometry used was stainless steel parallel plate geometry with 12 mm diameter. A solvent trap was used to prevent evaporation of the solvent. The viscoelastic properties of the water swollen gels were determined by measuring the changes in the storage modulus, G', and the loss modulus, G'', at 25 °C by applying a sinusoidal shear stress, τ. Two different viscoelastic tests were performed: (i) stress sweep experiments were carried out at a constant frequency of 1 Hz, and (ii) a frequency sweep experiment was performed at a constant stress of 5 Pa (located in the range of linear viscoelasticity) in the frequency range of 0.1–100 Hz. All the rheological measurements were performed in triplicate and the presented results are the average of those experiments. Apparent hydrogel network parameters were obtained from the storage modulus, G', and were derived from viscoelastic measurements and the following equations [25]:

$$\upsilon_e = \frac{G}{RT\varphi_2^{0.3\delta}} = \frac{E}{3RT\varphi_2^{0.3\delta}} \tag{2}$$

$$M_c = \frac{\rho}{\upsilon_e} \tag{3}$$

where G is the shear modulus, υ_e is the effective crosslink density, φ_2, is the polymer volume fraction, R is the universal gas constant ($m^3\,Pa\,K^{-1}\,mol^{-1}$), T is the temperature(K), ρ is the hydrogel density (kg/m^3) (calculated from hydrogel mass and geometric volume), and M_c is the molecular weight between crosslinks.

2.9. Drug loading

RM, NB, and VM were loaded into crosslinked polymer disks using a common solvent/solution absorption method. RM and NB (5 wt% each) were prepared in DMF,

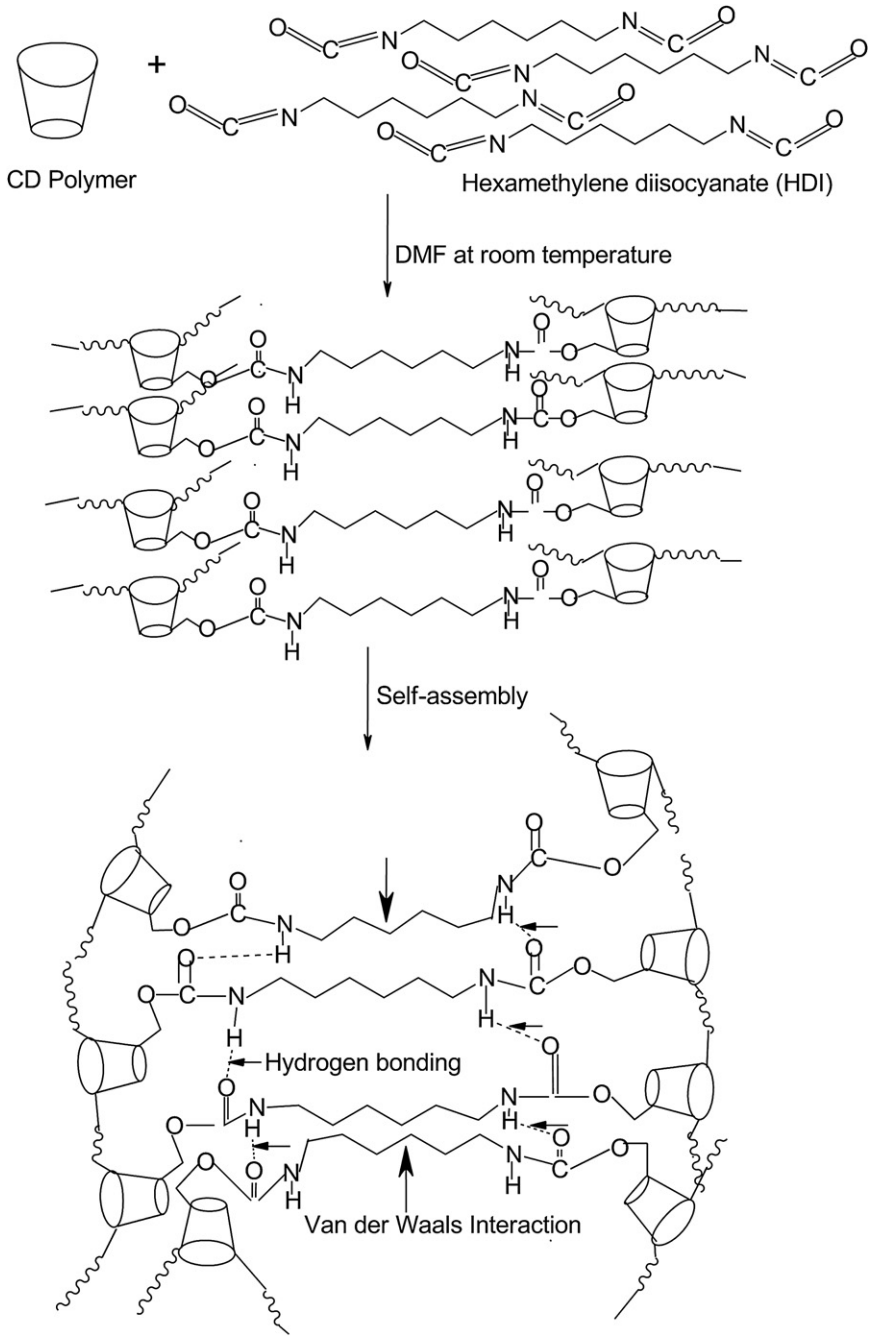

Fig. 1. Synthesis of HDI crosslinked CD-based gels.

whereas due to low DMF solubility, VM (5 wt%) was prepared in water. The drug was loaded into the disks by incubating the samples in the above solutions at room temperature for 4 days. The drug-loaded disks were first air-dried followed by vacuum drying at room temperature and used for in vitro drug release studies. Before immersion in the release medium, the samples were briefly washed 3 times with either a 1:1 DMF:water mixture, in the case of RM and NB, or pure water, used for VM, to remove surface-adsorbed drug. The coding scheme for the drug-loaded samples uses the following strategy: [saccharide monomer] – [crosslinker]([polymer:crosslinker ratio]) – [drug]. Specifically, the combinations evaluated in these studies are: Dex–LTI(1:0.16)-RM, Dex–LTI(1:0.32)-RM, CD–LTI(1:0.16)-RM, CD–LTI(1:0.32)-RM, CD–HDI(1:0.16)-RM, CD–HDI(1:0.32)-RM, Dex–LTI(1:0.16)-NB, Dex–LTI(1:0.32)-NB, CD–LTI(1:0.16)-NB,CD–LTI(1:0.32)-NB, CD–HDI(1:0.16)-NB, CD–HDI(1:0.32)-NB; Dex–LTI(1:0.16)-VM, Dex–LTI(1:0.32)-VM, CD–LTI(1:0.16)-VM, CD–LTI(1:0.32)-VM, CD–HDI(1:0.16)-VM, CD–HDI(1:0.32)-VM. The % of RM, NB and VM was determined spectrophotometrically at 473, 306, and 282, respectively, after extensive extraction in 1:1 DMF:water solution mixture. Loading percent was calculated as:

$$\%\text{loading} = W_{\text{drug}} / \left(W_{\text{sample}} + W_{\text{drug}}\right) \times 100$$

where W_{drug} and W_{sample} are weight of the drug and weight of the gel sample, respectively.

2.10. Drug loading for devices

For fabricated devices, we performed loading by placing each coated device in individual sample bottles containing different drugs (RM, NB, or VM) of the same concentrations as mentioned above for 4 days at room temperature. Samples were then removed from the loading solution, and excess solution was removed by gentle blotting with tissue paper and air drying, followed by vacuum drying at room temperature. The coding scheme for drug-loaded devices is as follows. For the polyester mesh (PM): PM–Dex–LTI(1:0.16)–RM, PM–CD–LTI(1:0.16)–RM, PM–Dex–LTI(1:0.16)–NB, PM–CD–LTI(1:0.16)–NB, PM–Dex–LTI(1:0.16)–VM, PM–CD–LTI(1:0.16)–VM. For the metal screws (MS): MS–Dex–LTI(1:0.16)–RM, MS–CD–LTI(1:0.16)–RM.

2.11. Drug release

For release studies, known weights of different drug-containing dry gel disks were placed in 20 mL sample bottles and 10 mL of phosphate buffer saline (PBS, pH 7.4) was added separately to each bottle. The bottles were placed in a shaking incubator at 37 °C with 100 rpm agitation. Aliquots (0.5 mL) were withdrawn periodically to determine drug concentration and, in all cases, equal volumes of buffer were immediately added to maintain a constant volume. RM, NB, and VM concentrations were determined spectrophotometrically at 473, 306, and 282 nm, respectively. Absorbance from blank samples (gels without drug) as a function of time was systematically measured and subtracted from the absorbance values of samples from drug-loaded gels. The amount of RM, NB, and VM released from the gels in dissolution medium, at a given time, was calculated using standard curves of each drug in corresponding buffers and expressed as a percentage of total drug content of the investigated gels. Each drug release experiment was repeated three times ($n = 3$).

2.12. Antibacterial activity of drug-loaded gels and drug-loaded devices

The antibacterial activity of the gel disks with and without antibiotic was determined against *Staphylococcus aureus* (*S. aureus* kindly provided by Dr. Ed Greenfield, Case Western Reserve University) using a nutrient agar method. Briefly, tripticase soy broth (15 g) and granulated agar (30 g) were added to 1 L of distilled water and autoclaved. The agar medium was then poured into Petri dishes and air-dried using sterile conditions. A constant volume (50 μL) of freshly grown *S. aureus* was added onto a tripticase soy agar plate, spread over the plate using a sterile glass spreader. Within 5 min, drug-loaded disks (5 mm in diameter) were placed on the inoculated plate and incubated overnight at 35 °C. The bactericidal activity was observed by visual inspection of the clearance of bacterial lawn as well as the size of the clearance as measured by calipers across an average diameter. Drug-loaded pellets were moved daily to a new lawn using the same process described above. This process was repeated for more than 30 days. The same procedure was adapted for the drug-loaded devices to test the bactericidal effect.

2.12.1. Statistical analysis

All data were processed using Microsoft Excel 2003 software and the results were produced as mean ± standard deviation of at least three experiments. Statistical analyses were performed using one-way ANOVA with Minitab (Minitab Inc. State College PA, U.S.A). A p-value smaller than 0.05 was considered statistically significant.

3. Results and discussion

3.1. Gel formation

In order to omit the heating process during gelation and to create gels capable of swelling in both water and organic solvents, we have developed a new room temperature gelation method. The general procedure for room temperature gelation is shown in Fig. 1. As a non-inclusion forming control, networks were also synthesized using dextran due to its comparable molecular weight and chemical similarity. Known weights of desired reactants (Table 1) were dissolved in DMF and samples were prepared from the resulting solutions. Gelation typically occurred within 8 h at room temperature, however the reaction was allowed to proceed for 48 h to ensure complete gelation. The described procedure we have adapted to make gels is typical in the synthesis of polyurethanes and PEG diisocyanates, but the reaction is very slow at room temperature [26]. Although these reactions can be accelerated by using a catalyst and higher temperatures, the method used here avoids secondary reactions, such as allophanate formation [27], which would complicate the structure.

3.2. FTIR analysis

The FTIR analysis of the hydrogels without drug (Fig. 2a and c) showed the typical signals corresponding to the formation of the urethane bond between cyclodextrin/dextran and LTI chains [8]. For all gels, absorption bands were observed around 3370 cm^{-1} (υNH), 1658 cm^{-1} (υC=O), and 1560 cm^{-1} (δNH), characteristic of the hydrogen bonded urethane groups. The absence of the signal at 2200 cm^{-1} (corresponding to the NCO stretching) indicated that these groups were reacted or hydrolyzed during washing. The FTIR spectral analysis of NB, shown in Fig. 2e, is similar to the spectrum reported elsewhere in the literature [28]. In this study, we are interested mainly in three specific peaks of NB: the stretching vibration of the carbonyl group at 1718 cm^{-1}, amide I at 1600 cm^{-1}, and aromatic group at 770 cm^{-1}. The indication of formation of the

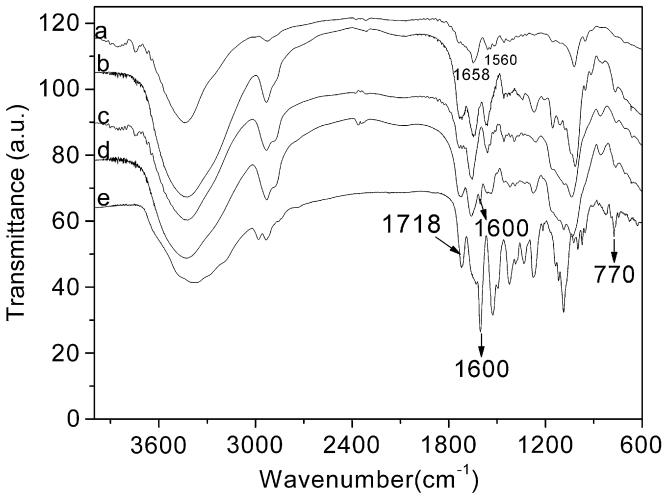

Fig. 2. FTIR spectra of a) LTI crosslinked dextran without NB (Dex–LTI (1.0.16)), b) LTI crosslinked dextran after loading with NB (Dex–LTI (1.0.16)–NB) c) LTI crosslinked CD without NB (CD–LTI(1:0.16)), d) LTI crosslinked CD after loading with NB (CD–LTI(1:0.16)–NB), e) Pure NB. Characteristic peaks of the hydrogen bonded urethane groups around 3370 cm^{-1} (υNH), 1658 cm^{-1} (υC=O), and 1560 cm^{-1} (δNH), indicates the formation of crosslinks by urethane linkage. The appearance of amide peak at 1600 and reduction of aromatic peak intensity in NB-loaded gels (Fig. 1d) indicate the formation of NB inclusion complex with CD.

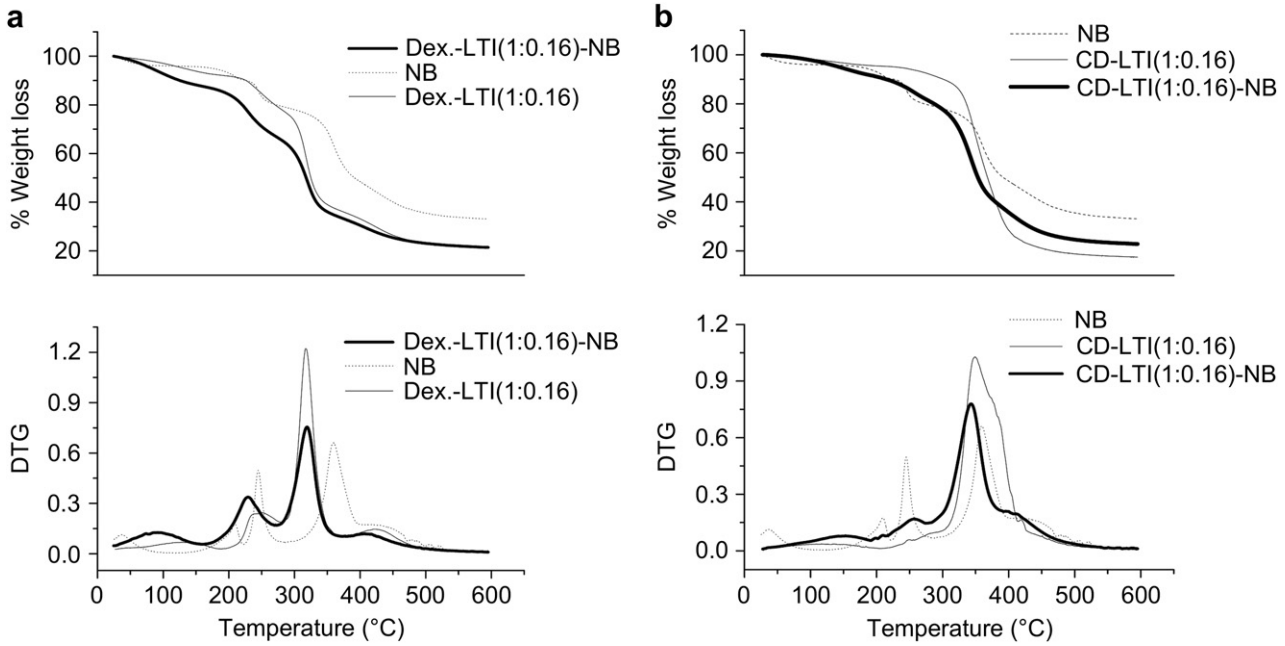

Fig. 3. TGA curves of a) Pure NB and dextran gels before and after NB loading, b) Pure NB and CD gels before and after NB loading. The disappearance of the first two onset degradation temperatures of NB in NB-loaded CD gels and the negative shift of onset degradation temperature of complexed CD compared to pure CD (Fig. 4b red line in DTG curve) indicate the formation of NB inclusion complex with CD gels.

NB:CD complex (CD–LTI(1:1)–NB) is shown in Fig. 2d, where it shows that the FTIR spectrum for the complex is almost similar to that of crosslinked CD alone (Fig. 2c), except the presence of amide I at 1600 cm^{-1} and aromatic peak at 770 cm^{-1}. The presence of amide I and reduced peak intensity in the aromatic region indicates the formation of the inclusion complex. Presumably, the complexation occurs with the alkyl chain end (hydrophobic) of NB present in the CD cavity and the amide end (hydrophilic) present outside the cavity.

3.3. Thermo-gravimetric analysis (TGA)

Thermo-gravimetric analysis (TGA) and differential scanning calorimetry (DSC) have been carried out to know the thermal properties and formation of inclusion complex between drug and CD. TGA and DSC data of RM loaded gels are presented in Supplementary data (Figs. S1 and S3). Here NB-loaded gels TGA results are presented. The study of the gels by thermogravimetry shows that they have high thermal stability. The thermal stability of CD-based gels was higher than that of dextran-based gels. Fig. 3a and b shows the thermo-gravimetric curves (top) and their first derivative of TG traces (DTG) (bottom) for the gels, Dex–LTI(1:0.16) and CD–LTI(1:0.16), respectively, both with and without drug. The thermal degradation of these gels is a complex process involving several overlapped stages. The derivatives study of the thermo-gravimetric curves shows a minimum close to those obtained for pure gels and pure drug. It is therefore most likely that the degradation of these components plays a major role in the entire degradation process. For example, there were three onset degradation temperatures for NB (Fig. 3a and b, Table 2). However, when NB was loaded in to dextran gels, the first and second onset degradation temperatures of NB appeared as a single peak in between the first and second onset degradation temperatures of pure NB. However, the third onset degradation temperature of NB is after the gel degradation temperature; therefore, it is not visible in the degradation curves of drug-loaded dextran. In the case of NB-loaded CD gels, the first and second onset degradation temperatures of NB shifted to higher temperatures as shown in Fig. 3b and Table 2. This clearly indicates that CD:NB complexation has been occurred. In addition it is also observed that the degradation temperature of complexed CD-based gels decreases when compared to pure CD gels which is in agreement with the previously published results of macromer:CD complexation [29]. It is also well known in protein chemistry that the hydrogen bonding melts with heating and hydrophobic interactions become stronger initially upon heating, [30] which supports the TGA results of drug-loaded control gels and CD-based gels. In the case of control gels, the interaction between drug and dextran may be hydrogen bonding that melts upon heating thereby the drug in dextran gels decomposes similar way to that of pure drug. In the case of drug-loaded CD gels, the complexed drug is decomposing at higher temperatures than the free drug, which may be due to strengthening of hydrophobic interaction that has already been formed during complexation.

3.4. Swelling studies of the gels

Equilibrium swelling studies have been conducted in water and DMF for CD-based gels whereas water and DMSO were used for the dextran (control) gels, since dextran gels do not swell in DMF. Fig. 4a shows the swelling ratios of CD-based gels and Fig. 4b for dextran gels. As shown in Fig. 4a and b, swelling is higher in organic

Table 2
Onset degradation temperatures of NB, NB-loaded gels, and pure gels.

Sample code	Onset degradation temperatures
NB	207, 243, 360
Dex–LTI(1:0.16)	243, 318
Dex–LTI(1:0.16)–NB	227, 318
CD–LTI(1:0.16)	350
CD–LTI(1:0.16)–NB	255, 343
CD–HDI(1:0.16)	355
CD–HDI(1:0.16)–NB	313, 340

solvents for both CD gels and dextran gels, compared to water, for all gels studied. The higher swelling of CD gels in DMF and dextran gels in DMSO could be attributed to the organic solvent being more compatible with the polymer network than water. The quantitative swelling ratios of different gels in different solvents are useful in deciding which solvent can be used to dissolve the drug in order to load it into the gels. Most of the drugs that were chosen for this study were fully soluble in DMF and DMSO, except for Vancomycin. However, Vancomycin could still be used here since all the gels possess sufficient swelling in water. The purpose of conducting the swelling studies in the above solvents was to know the solvent uptake ability of the gels. This information could be useful to increase the loading efficiency of the drugs in different gels. From Fig. 4a and b it is evident that all the gels that were prepared, possess swelling ability in both water and polar organic solvents, which spurred the ability to load both water soluble and water insoluble drugs. The synthetic gels developed so far either swell in water or nonpolar solvents [31–33], but typically not both.

3.5. Viscoelastic measurements

The type and concentration of the crosslinkers were varied to assess the effects of crosslink density on gel properties. Viscoelastic properties were explored by both frequency and stress sweep experiments. At first storage and loss moduli, G' and G'', respectively, were measured as a function of angular frequency at a fixed stress of 5 Pa. Fig. 5a shows the variation of equilibrium moduli for all the crosslinked gels with regard to angular frequency. One of the general features observed for the two different gels (CD–HDI(1:0.16) and CD–LTI(1:0.16)) is the pronounced plateau of G' in the full frequency range and a G'' which is considerably smaller than the storage moduli (3–5 orders of magnitude). However, in the case of CD–HDI(1:0.32) the G' is constantly increasing, which may be due to a greater loss of water during the experiment leading to stiffening of the gel. The greater loss of water in CD–HDI(1:0.32) compared to other gels could be due to its greater hydrophobicity, reducing its hydration capacity. This feature of higher G' compared to G'' indicates the formation of strong and rigid gels. Fig. 5a shows a more than two-fold increase of storage modulus is observed upon doubling the crosslinker concentration in the case of HDI as crosslinker. Interestingly, the HDI-based crosslinked gel exhibited higher storage modulus values when compared to LTI crosslinked gel even though the crosslinker concentration is the same. This can be attributed to spatial arrangement/aggregation of hexamethylene chains in such a way to form stronger interactions including H-bonding and hydrophobic interactions (Fig. 1). The higher modulus values observed for HDI-based gels can be due to increased crosslinking density and decreased M_c values (Table 3), which could be due to a more flexible, linear hydrophobic crosslinker which may have hydrophobic attraction towards CD that can reduce the steric hindrance and facilitate crosslinking. Biomaterials with moduli in the kPa range are of widespread interest because many native tissues have moduli in this range [34]. Therefore, an added benefit of the materials in this study is that their mechanical properties can be appropriately tuned for tissue engineering applications.

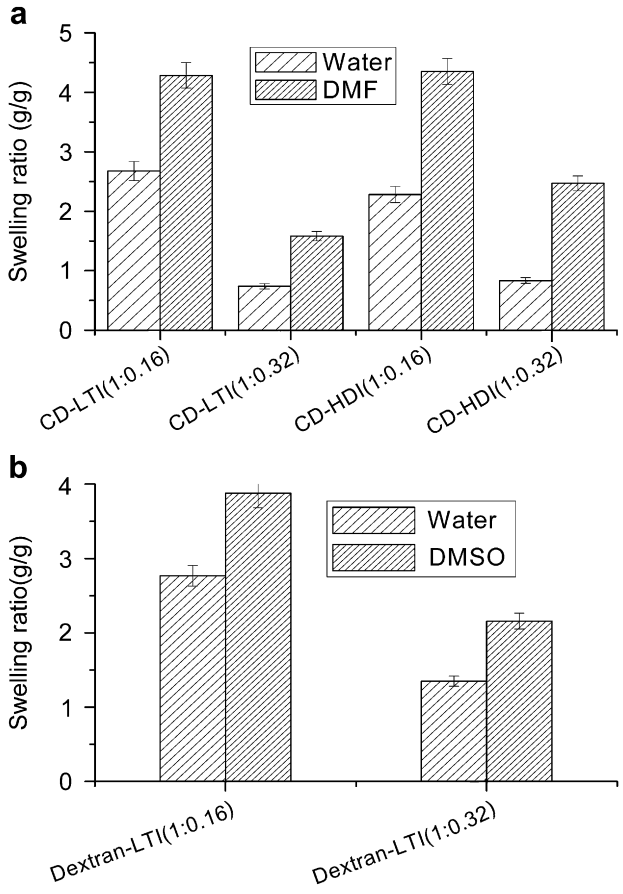

Fig. 4. Effect of LTI and HDI content on swelling ratio of the different gels in different solvents. a) Swelling ratio of CD-based gels in water and DMF, b) Swelling ratio of dextran gels in water and DMSO. All gels had a higher swelling ratio in organic solvents than in water. The swelling ratio decreased with increasing concentration of crosslinker. Experiments are done in triplicate ($n = 3$) and error bars represent ±standard deviation.

Stress sweep experiments were also performed on the three gels (CD–HDI(1:0.16), CD–HDI(1:0.32) and CD–LTI(1:0.16)) and are shown in Fig. 5b. At the beginning of the experiment, the storage modulus, G', exhibited a constant value under the shear stress applied. However, when the shear stress exceeded 3000 Pa, the storage modulus gradually started decreasing (Fig. 5b inset). The decrease of G' at higher stresses could be due to squeezing of water from bulk gel to the surface of the gel that may lubricate the material and therefore lead to a decrease in modulus. More recently, self-assembled CD-based gels have been developed for drug delivery applications, however, they dissociate at very low stress values [35,36].

3.6. Network and interaction parameters for crosslinked CD-based gels

The polymer–water interaction parameter (χ) in a swollen hydrogel was determined from the following equation [25]

$$\chi = \frac{-\left[\ln(1-\varphi_2)+\varphi_2+\upsilon_e V_1\left(\varphi_2^{0.33}-0.5\varphi_2\right)\right]}{\varphi_2^2} \quad (4)$$

where V_1 is the molar volume of water (1.8×10^{-5} m^3/mol). Table 3 shows the network and interaction parameters of the current gels. The values of G', ν_e, and χ increased with increased amounts of HDI in the case of HDI crosslinked gels. However, smaller values for G', ν_e, and χ were observed for CD–LTI(1:0.16) compared to the CD–HDI(1:0.16) crosslinked gel even though the crosslinker concentration is the same. The smaller χ value of CD–LTI(1:0.16) as compared to CD–HDI(1:0.16) demonstrates that water becomes a "better solvent" for LTI-based gels, which could be due to more hydrophilic nature of LTI compared to the HDI crosslinker.

This can also be explained in terms of polymer volume fraction (φ_2), the polymer volume fraction of the gels decreased with

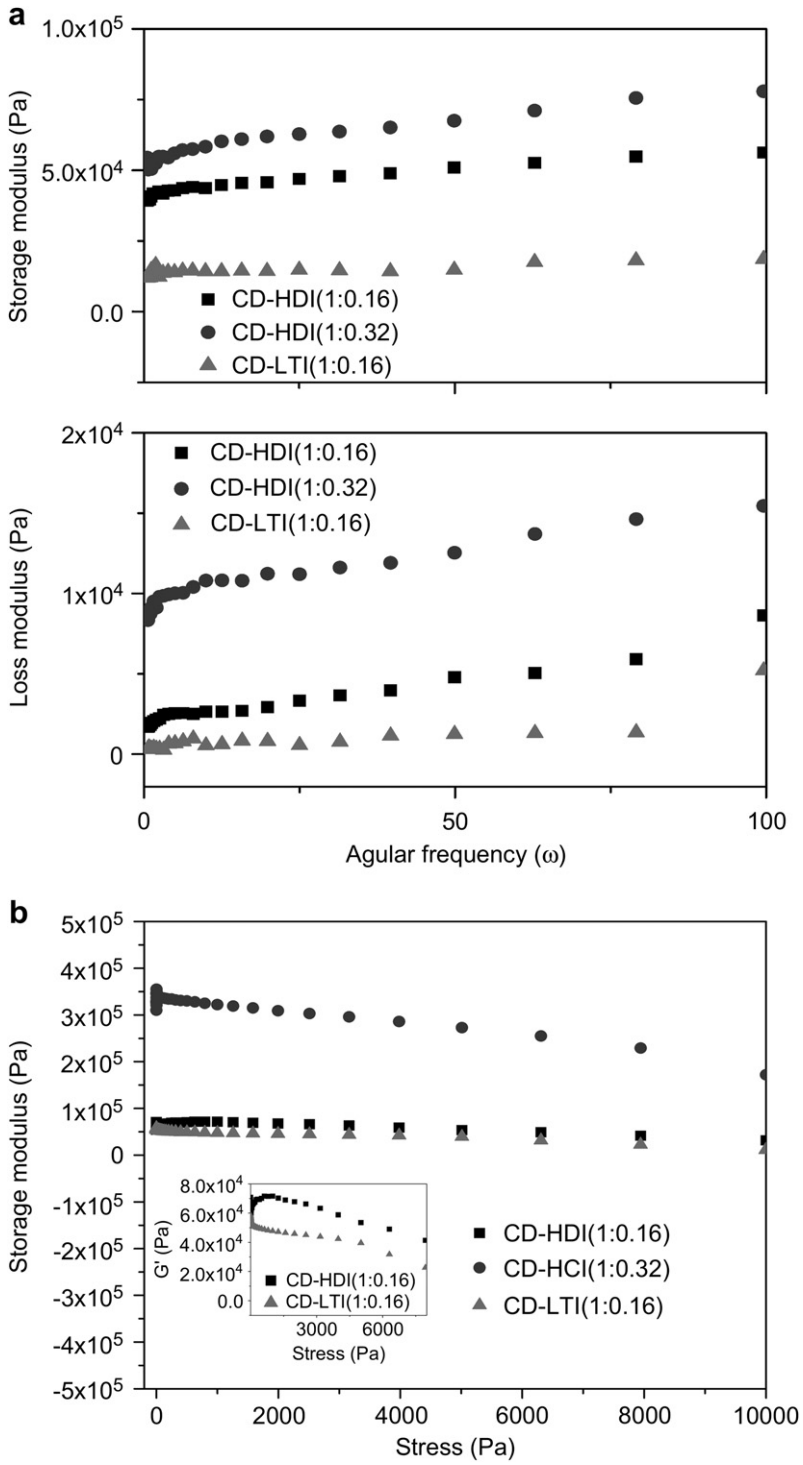

Fig. 5. Viscoelastic measurements of crosslinked CD gels. a) Frequency dependence of dynamic storage modulus (G′) and loss modulus (G″) with type and crosslinker concentration, b) Stress dependence of dynamic storage modulus (G′) with type and crosslinker concentration. A significant variation of modulus just by changing the type and concentration of crosslinker.

decreasing crosslinker concentration in case of HDI crosslinked gels, this can be due to the decreased crosslinker concentration, which increases the hydrophilicity and leads to higher equilibrium water content (*Q*) and, hence, a lower volume fraction. However, when comparing CD–HDI(1:0.16) to CD–LTI(1:0.16), the φ_2 value is less for the LTI crosslinked gel, which is due to a more hydrophilic crosslinker that leads to more equilibrium swelling and therefore a lower φ_2 is observed.

3.7. Scanning electron microscopy (SEM)

To evaluate visual insights into the surface morphology of freeze dried hydrogels, we took SEM images of the gels CD–LTI(1:0.16), CD–LTI(1:0.32), CD–HDI(1:0.16), CD–HDI(1:0.32), and Dex–LTI(1:0.32). Fig. 6a and b shows the surface morphology of CD gels crosslinked with two different concentrations of LTI. The surface morphology of CD–LTI(1:0.16) gels (Fig. 6a) possesses fairly uniform

Table 3
Mechanical properties and network parameters for the CD-based gels.

Sample code	φ_2	E' (MPa)	G' (MPa)	ν_e (mol/m^3)	M_c (kg/mol)	χ
CD–LTI(1:0.16)	0.423	0.0434	0.01447	7.764	113.41	0.708
CD–HDI(1:0.16)	0.542	1.3116	0.04372	21.59	41.466	0.812
CD–HDI(1:0.32)	0.651	1.7181	0.05727	26.63	34.689	0.947

pores throughout the surface. However, in the case of CD–LTI(1:0.32) the morphology has been considerably changed and possesses no apparent pores when imaged at the same magnification. Fig. 6b–d shows the surface morphology of CD gels crosslinked with two different concentrations of HDI. The morphology of gels made with lower HDI crosslinker concentration resulted in a large pore diameter resembling a rippled texture (Fig. 6c). However, the morphology of the gels made with higher HDI crosslinker exhibits a largely uniform smooth surface with occasional small, porous islands. These porous islands may be responsible for absorbing drug molecules from the solution and may distribute the drug throughout the bulk network structure. Fig. 6e shows the surface morphology of the control gel (Dex–LTI(1:0.32) possessing a porous, yet non-uniform network. The comparison of LTI and HDI crosslinked samples demonstrated that changing the crosslinker concentration and type of the crosslinker promoted significant changes in the surface morphology of the gels.

3.8. Morphology of the gel-coated mesh

The goal of this work is the development of gels able to coat medical devices, such as hernia repair meshes, under mild conditions with the potential capacity of improving integration of the device. CD-based coatings on medical devices have previously been reported, but those resulted in a rough surface [13]. Here, we have developed elastic gels (Fig. 5) with the aim of achieving a smooth surface after coating on the devices. Fig. 7a shows the surface morphology of a Dex–LTI(1:0.16) coated mesh and Fig. 7b is CD–LTI(1:0.16) coated one. The morphology of the dextran-coated mesh revealed that the gel coating does not uniformly cover the

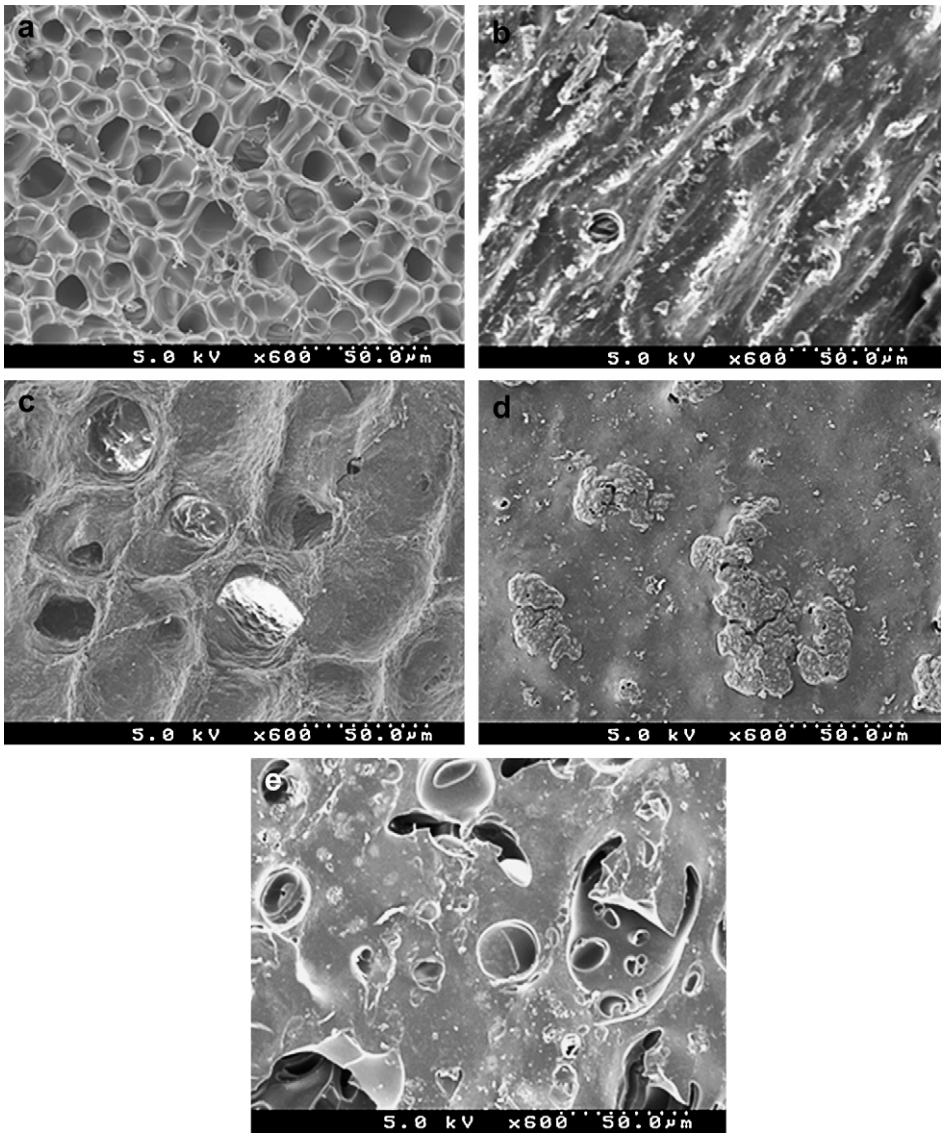

Fig. 6. SEM micrographs showing the top view of different lyophilized samples. a) CD–LTI(1:0.16); b) CD–LTI(1:0.32); c) CD–HDI(1:0.16); d) CD–HDI(1:0.32); e) Dex–LTI(1:0.32); .The surface morphology of the LTI crosslinked CD is porous at lower crosslinker concentration (a) and rigid (b) at higher crosslinker concentration. The HDI crosslinked CD is porous micro-fibrous texture (c) at lower crosslinker concentration and smooth and porous islands (d) at higher crosslinker concentration. The LTI crosslinked dextran is porous and rigid morphology (e). Morphology depends on the type and crosslinker concentration.

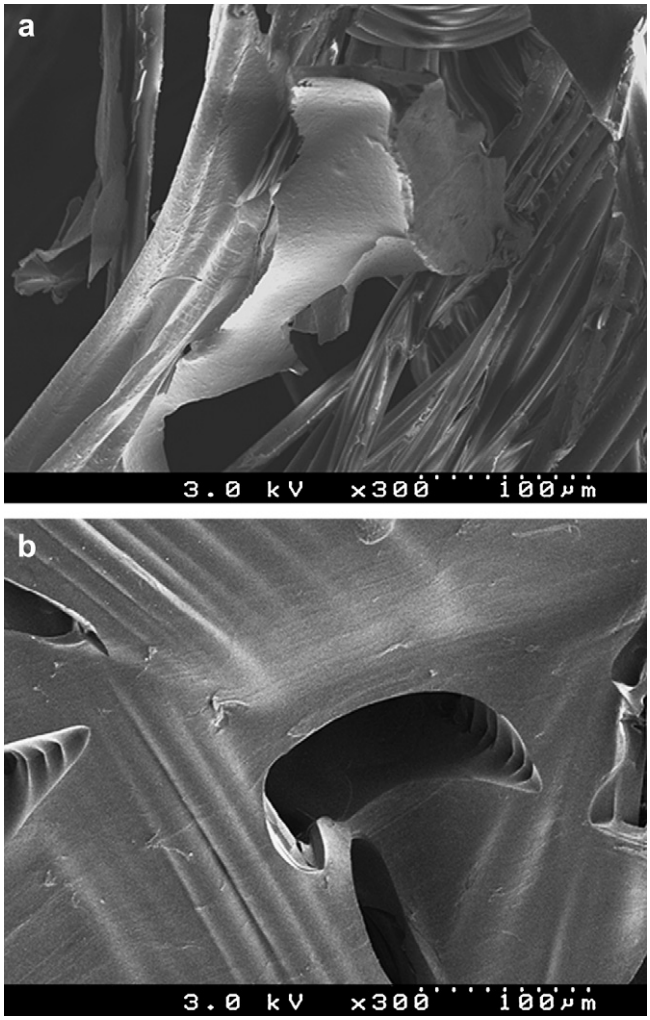

Fig. 7. SEM micrographs showing the top view of gel-coated Parietex™ mesh after air drying. a) PM–Dex–LTI(1:0.16); b) PM–CD–LTI(1:0.16). Dextran-coated mesh appears to be delaminating from the mesh (a), however, a smooth uniform film has been formed in the case of CD gel-coated mesh (b).

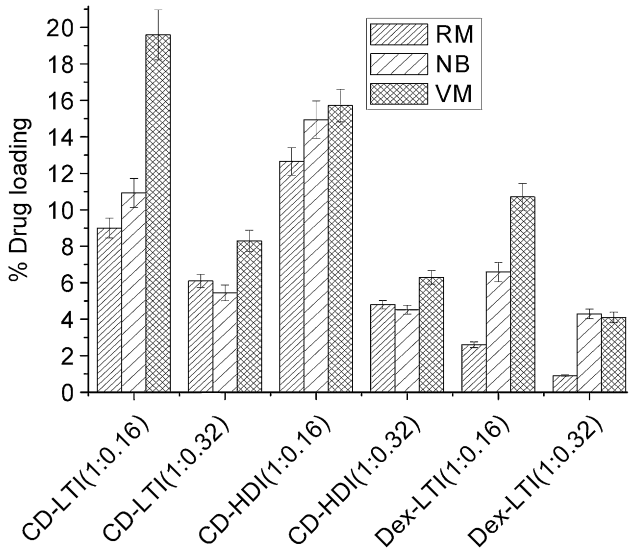

Fig. 8. Effect of crosslinker (LTI or HDI), crosslinking ratio, and drug choice on loading efficiency. Crosslinked CD-based gels showed higher drug loadings compared to dextran gels; however in all cases increasing crosslinker ratio led to a decrease in loading. The higher water solubility of Vancomycin led to increased drug loading in all the gels. Experiments are done in triplicate ($n = 3$) and error bars represent ±standard deviation.

device and poor adhesion is apparent, with gel delamination from the mesh, which may be due to poor wetting of the dextran gel to the mesh surface. However, in the case of the CD-based gel, a smooth coating was observed throughout the surface, indicating that it easily wets the surface and forms a uniform thin film coating on it. We also coated orthopedic fixation screws (Kirschner wires) with the above gels. In the case of metal screws, both dextran and CD gels coated well and formed uniform coatings (Supplementary data Figs. S5 and S6), which may be due to roughness of the screws that allows the gel solution to spread and wet the complete surface and form good adhesion through mechanical interlocking adhesion mechanism.

3.9. Loading efficiency

From the swelling studies, it was shown that the gels swell in water as well as in organic solvents. This ability is useful for loading

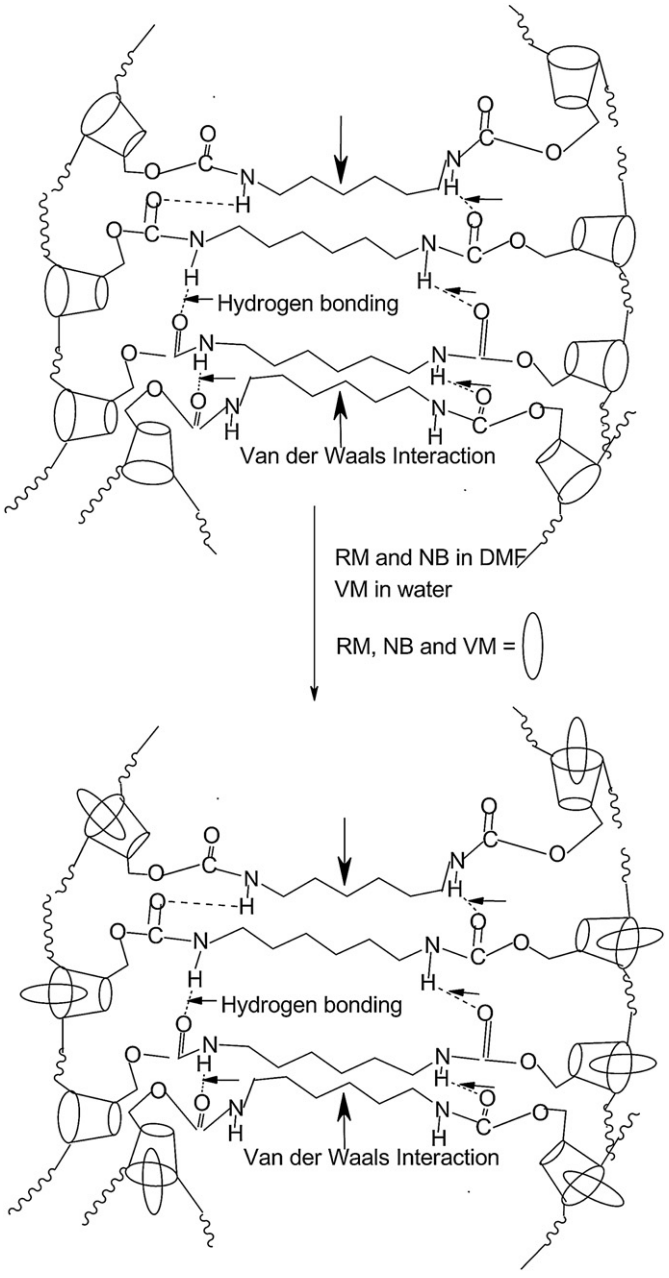

Fig. 9. Drug loading and complexation procedure in HDI crosslinked gels.

both water and organic solvent soluble drugs. Solution absorption methods were employed to load the drugs into the crosslinked gels. The percent loading in the different gels is displayed in Fig. 8. Unlike our previous report [8] where the percent loading did not exceed more than 3.5% in any of the prepared gels, here a significant improvement in drug loading efficiency is observed irrespective of the solvent in which the drug was solubilized. The higher drug loading may be due to higher swelling ability of the gels in both water and organic solvents. Vancomycin loading efficiency is higher in all the gels that have been investigated compared to the other two drugs, which may be due to the fact that VM is highly water soluble. Therefore, drug loading was carried out in water for VM, which enable the improvement of loading efficiency because water is a good solvent to load the drugs into CD-based gels [9]. The higher loading of VM may also be due to the presence of two glucose units present in the VM structure that may enhance the compatibility between VM and the gel thereby facilitating more loading. It is also observed from Fig. 8 that CD–HDI(1:0.16) has a higher loading efficiency for all three drugs when compared to other gels even though the swelling is similar to that of CD–LTI(1:0.16). The higher loading of drug into CD–HDI(1:0.16) is presumably attributed to spatial arrangement of CDs (Fig. 9) allowing easier formation of an inclusion complex with drug molecules.

3.10. Antibiotics release studies

In the case of other hydrogels, regulation of drug release depends on several parameters such as solubility of the drug, crosslinking density of the hydrogel network, and sometimes degradation of the gel network. However, the release of the drug from the CD-based gels additionally depends on the molecular interaction between drug and the CD cavity, thereby delaying the release of drug from the CD-based systems compared to normal, diffusion-only hydrogels. The combination of antibiotics and CDs has been reported in the literature in an effort to improve the

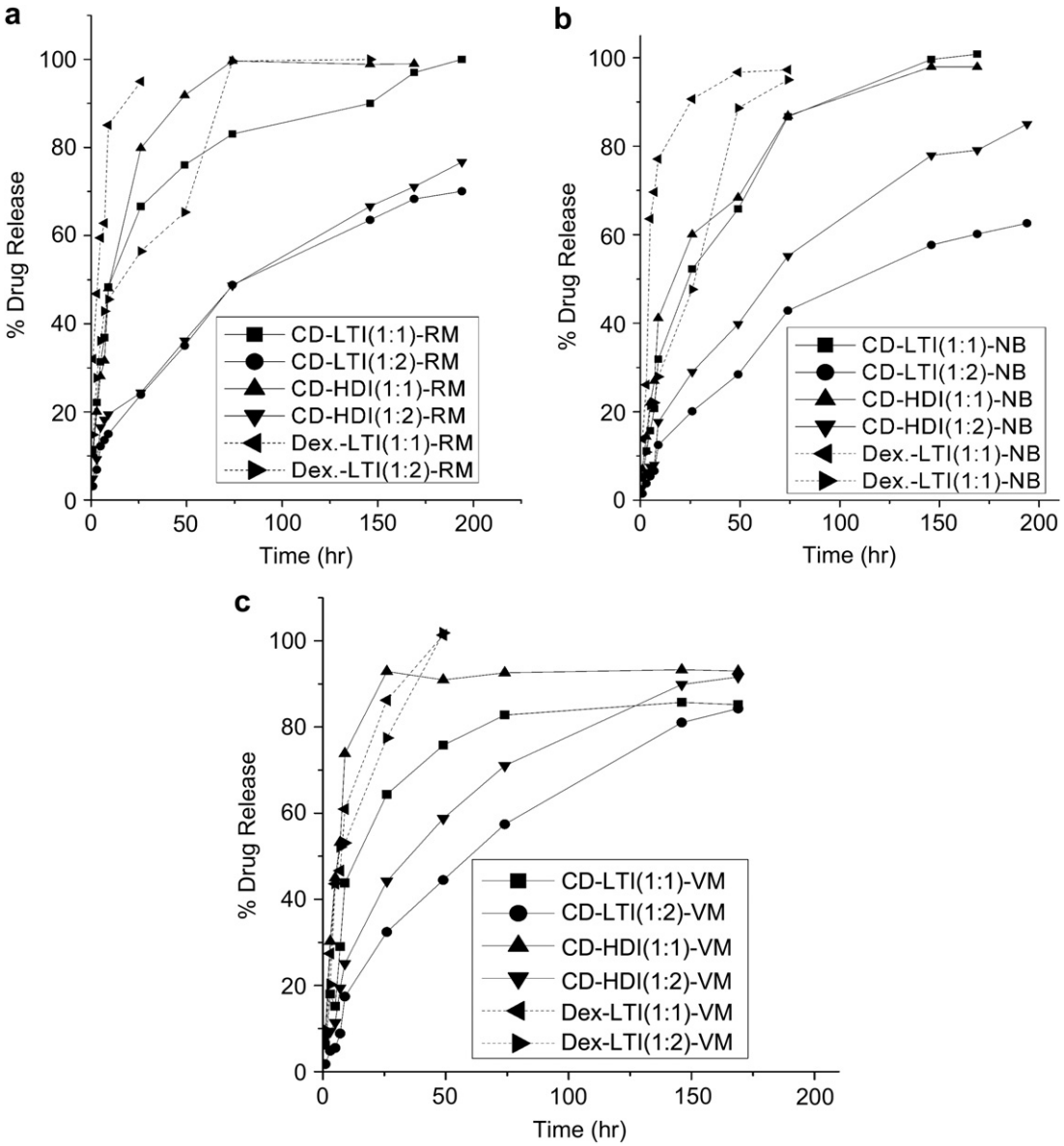

Fig. 10. Effect of the crosslinker content and type on drug release from dextran and CD-based gels in PBS, pH 7.4 at 37 °C. a) RM release from dextran and CD gels, b) NB release from dextran and CD release, c) VM release from dextran and CD gels. All drugs released rapidly from dextran-based gels. However, drug release from CD-based gels is more linear and sustained. Increasing crosslinker concentration led to a slower release rate.

solubility, stability, and sustained delivery of the antibiotics [37,38]. In this study, we have chosen dextran-based gels as a control because they are chemically similar and have comparable molecular weight to that of the CD pre-polymer. The release of drugs from the gel disks was characterized over a 200 h period, and the percent release of the drugs from these samples is shown in Fig. 10a–c. As expected, dextran gels, which do not possess a hydrophobic cavity, exhibited in all cases non-linear release with a rapid initial phase (burst), with the amount of drugs released decreasing rapidly with time. As mentioned above, the regulation of drug release, in the case of the control gels (dextran), depended on the solubility of the drug, network swelling, and crosslink density. Increasing the crosslinker concentration resulted in a more dense packing of chains in the gels, and thus slowed the release of drugs when compared with gels prepared with a lower concentration of crosslinker. However, in the case of CD gels, the drug release depended on the crosslinking concentration as well as the complexation of drugs with CD. Complexation acts as a rate-limiting barrier to the drug, enabling better control of drug release and allowing a steady, sustained release. As can be seen in Fig. 10a–c, although the same amount of crosslinker was used to prepare both the dextran and CD gels, the release was slower in the case of the CD gels for all of the drugs studied, indicating that inclusion complexes were formed irrespective of the hydrophilicity/hydrophobicity of the drug. It is also observed from Fig. 10a–c that the VM released faster than RM and NB. The faster release of VM may be due to higher solubility of drug in water.

3.11. Antibacterial activity of gels

Although the drug release studies presented above demonstrate that numerous antibiotics can be released from the CD-based hydrogels, confirmation is needed that released RM, NB, and VM maintain their ability to kill bacteria. To confirm this, drug-loaded 5 mm diameter gel disks of all formulations were placed in different agar plates containing grown *S. aureus*, the most common species of bacteria associated with human device infection. The choice of the above three antibiotics was based on their wide application and effectiveness in the biomedical field. The zones of inhibition, defined as the distance between the test disk and the edge of bacterial growth (recorded in mm), and the number of days cleared are presented in Fig. 11a–c. As expected, the zone of inhibition of control gels (dextran gels) showed higher zones of inhibition at first and gradually reduced and became zero within 5–15 days, irrespective of the drug that was loaded into them. However, the zone of inhibition for CD gels remained constant and larger throughout the study for RM and NB containing gels, lasting somewhat shorter in the case of hydrophilic VM. The difference in the diameter of the zone of inhibition between the dextrose and CD-based gels can be attributed to the burst release of antibiotics seen in diffusion-based delivery systems initially (such as dextran gels) as compared to affinity-based release (CD gels).

3.12. Device coating, drug loading and antibacterial activity of the drug-loaded devices

For device coating applications, particularly for sensitive devices such as hernia repair meshes, we have investigated a mild approach to coat devices (Fig. 7) with crosslinked CD. We have used both LTI and HDI crosslinkers that crosslink the CD without use of harsh conditions. This polymer system allows us to study the effect of gel-coated and drug-loaded devices specifically in regards to antibacterial activity. Two devices, hernia repair mesh (polyester mesh resembling the chemical composition of vascular graft) and metal screws, were coated with CD–LTI(1:0.16) and Dex–LTI(1:0.16) gels.

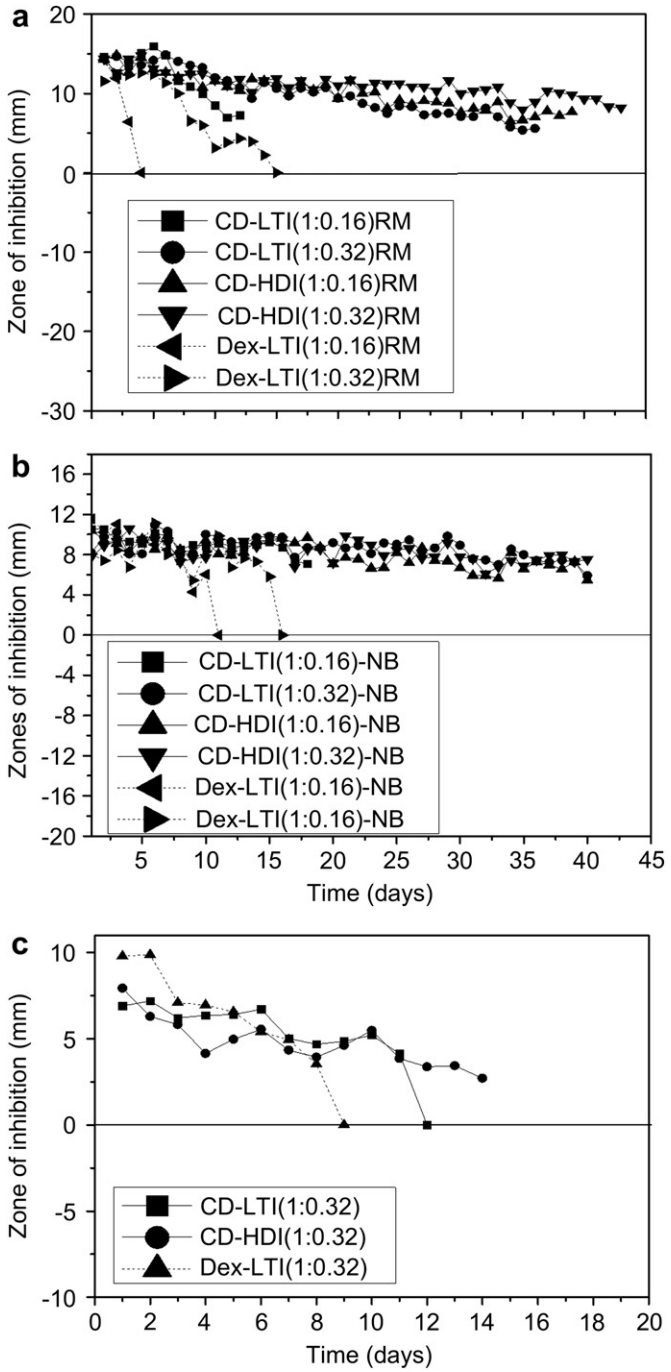

Fig. 11. The capacity of delivered antibiotics to clear a lawn of *S. aureus* and form a zone of inhibition. Cleared zone size versus number of days cleared is plotted, expressing the kinetics of bactericidal activity for each of the drug delivery platforms tested. a) Zones of inhibition of RM containing dextran and CD gel discs; b) Zones of inhibition of NB containing dextran and CD gel discs; c) Zones of inhibition of VM containing dextran and CD gel discs. The dextran gels were incapable of clearing bacteria beyond 15 days whereas CD-based gels continuously showed a zone of inhibition beyond 40 days in the case of RM and NB. Gels releasing hydrophilic VM were not able to clear lawns for as long as gels with hydrophobic drugs.

All three drugs were tested loaded into the coated mesh, but only RM was tested with the coated screws. The time dependence of the bactericidal effect of the drug-loaded devices as a function of the amount of organism cleared was examined. The zones of inhibition (recorded in mm) around the antibiotic containing gel-coated mesh disks are presented in Fig. 12a. CD coated mesh disks, PM–CD–

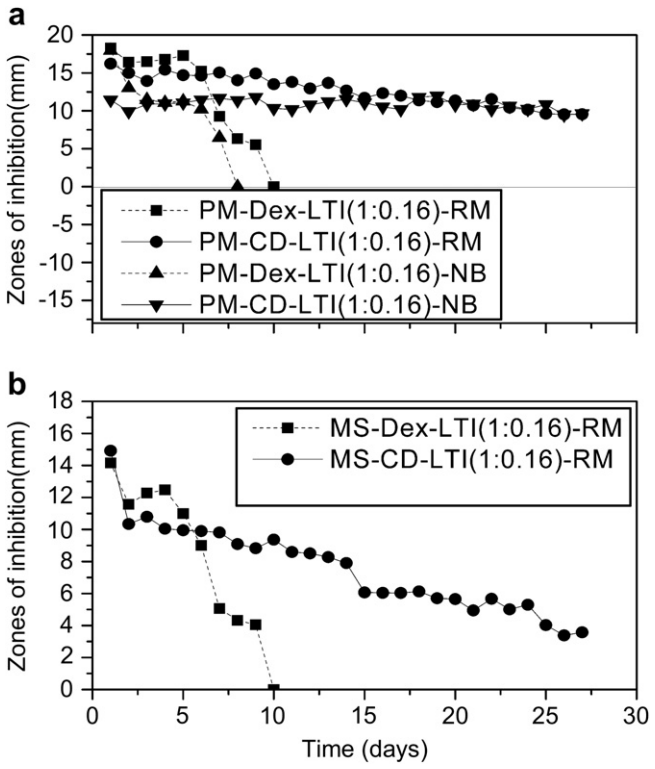

Fig. 12. The capacity of delivered antibiotics to clear a lawn of *S. aureus* and form a zone of inhibition. Cleared zone size versus number of days cleared is plotted, expressing the kinetics of bactericidal activity for each of the drug delivery platforms tested. a) RM and NB containing gel-coated mesh; b) RM containing gel-coated screw. The dextran gels were incapable of clearing bacteria beyond 15 days whereas CD-based gels continuously showed a zone of inhibition beyond 28 days.

LTI(1:0.16)–RM and PM–CD–LTI(1:0.16)–NB, showed effective bactericidal activity in terms of zone of inhibition (Supplementary data Fig. S4) against *S. aureus* for over a month with daily application to a lawn of freshly grown bacteria. However, dextran-coated mesh disks, PM–Dex–LTI(1:0.16)–RM and PM–Dex–LTI(1:0.16)–NB, showed bactericidal activity on *S. aureus* for only 8–10 days (Fig. 12a). Similar to the gels discussed above, dextran-coated disks showed larger zones of inhibition initially, which then reduced drastically and fell to no zone of inhibition within 10 days. However, CD coated samples showed fairly constant values of zones of inhibition over a long period of time. This bactericidal effect was observed to extend beyond 30 days in the case of CD coated gels.

Antibiotic containing metal screws coated with gels were evaluated for their antibacterial activity and results are presented in Fig. 12b. The observations with screws coated with dextran gels or CD gels containing antibiotics, (Fig. 12b) were similar to that of the gel-coated mesh disks (Fig. 12a). The difference in the diameter of the zone of inhibition between the dextran and CD coated screws can again be attributed to the burst release of antibiotics seen in diffusion-based delivery systems (such as dextran gels) as compared to affinity-based release (CD gels).

4. Conclusions

Affinity-based drug delivery coatings were made under mild conditions and with no external agents, and could be coated on devices ranging from polymer meshes to metal screws. These cyclodextrin-based gels, able to swell in both water and DMF, showed substantial improvements in drug loading and mechanical properties to existing CD polymers. Control gels (dextran-based networks) were also synthesized to compare with the cyclodextrin gels specifically in terms of morphology, swelling, drug loading, release, and bactericidal effect. The drug loading and release in dextran gels, relying chiefly on diffusion for drug release, depend on the type and concentration of crosslinker, and solubility of drug. However, in the case of affinity-based CD gels, drug loading and regulation of drug release additionally depended on the complexation ability of CD with the drug molecules, leading to delivery of drug molecules in a longer, more linear sustained manner. Therefore, CD-based gels are expected to be useful as coating materials for a broad range of biomedical devices where high tissue integration and sustained drug release are distinct advantages in monitoring the fate of implanted devices.

Acknowledgements

The authors would like to acknowledge support from the Coulter-Case Translation and Innovation Partnership.

Appendix A

Figure with essential colour discrimination. Certain figures in this article, particularly Figs. 3, 5, 10–12, are difficult to interpret in black and white. The full colour images can be found in the online version, at doi:10.1016/j.biomaterials.2009.11.087.

Appendix B. Supplementary data

Supplementary data associated with this article can be found, in the online version, at doi:10.1016/j.biomaterials.2009.11.087.

References

[1] Calvert P. Hydrogels for soft machines. Adv Mater 2009;21(7):743–56.
[2] Peppas N, Hilt J, Khademhosseini A, Langer R. Hydrogels in biology and medicine: from molecular principles to bionanotechnology. Adv Mater 2006;18(11):1345–60.
[3] Coughlan D, Quilty F, Corrigan O. Effect of drug physicochemical properties on swelling/deswelling kinetics and pulsatile drug release from thermoresponsive poly(N-isopropylacrylamide) hydrogels. J Control Release 2004;98(1):97–114.
[4] Rodriguez-Tenreiro C, Alvarez-Lorenzo C, Rodriguez-Perez A, Concheiro A, Torres-Labandeira J. New cyclodextrin hydrogels cross-linked with diglycidylethers with a high drug loading and controlled release ability. Pharm Res 2006;23(1):121–30.
[5] Tewes F, Brillault J, Couet W, Olivier J. Formulation of rifampicin–cyclodextrin complexes for lung nebulization. J Control Release 2008;129(2):93–9.
[6] Rodriguez-Tenreiro C, Alvarez-Lorenzo C, Rodriguez-Perez A, Concheiro A, Torres-Labandeira J. Estradiol sustained release from high affinity cyclodextrin hydrogels. Eur J Pharm Biopharm 2007;66(1):55–62.
[7] dos Santos J, Alvarez-Lorenzo C, Silva M, Balsa L, Couceiro J, Torres-Labandeira J, et al. Soft contact lenses functionalized with pendant cyclodextrins for controlled drug delivery. Biomaterials 2009;30(7):1348–55.
[8] ThimmaReddy T, von Recum HA, Komiyama M. Cyclodextrin complexation for affinity-based antibiotic delivery. Macromol Biosci 2009;Sep 8 [Epub ahead of print].
[9] Asanuma H, Hishiya T, Komiyama M. Tailor-made receptors by molecular imprinting. Adv Mater 2000;12(14):1019–30.
[10] Blanchemain N, Haulon S, Boschin F, Marcon-Bachari E, Traisnel M, Morcellet M, et al. Vascular prostheses with controlled release of antibiotics – part 1: surface modification with cyclodextrins of PET prostheses. Biomol Eng 2007;24(1):149–53.
[11] Blanchemain N, Haulon S, Boschin F, Traisnel M, Morcellet M, Martel B, et al. Vascular prostheses with controlled release of antibiotics – Part 2. In vitro biological evaluation of vascular prostheses treated by cyclodextrins. Biomol Eng 2007;24(1):143–8.
[12] Blanchemain N, Haulon S, Martel B, Traisnel M, Morcellet M, Hildebrand H. Vascular PET prostheses surface modification with cyclodextrin coating: development of a new drug delivery system. Eur J Vasc Endovasc 2005;29(6):628–32.
[13] Blanchemain N, Laurent T, Haulon S, Traisnel M, Neut C, Kirkpatrick J, et al. In vitro study of a HP gamma-cyclodextrin grafted PET vascular prosthesis for application as anti-infectious drug delivery system. J Incl Phenom Macro 2007;57(1–4):675–81.
[14] El Ghoul Y, Blanchemain N, Laurent T, Campagne C, El Achari A, Roudesli S, et al. Chemical, biological and microbiological evaluation of cyclodextrin finished polyamide inguinal meshes. Acta Biomater 2008;4(5):1392–400.

[15] Blanchemain N, Laurent T, Chai F, Neut C, Haulon S, Krump-konvalinkova V, et al. Polyester vascular prostheses coated with a cyclodextrin polymer and activated with antibiotics: cytotoxicity and microbiological evaluation. Acta Biomater 2008;4(6):1725–33.
[16] Mhlanga S, Marnba B, Krause R, Malefetse T. Removal of organic contaminants from water using nanosponge cyclodextrin polyurethanes. J Chem Technol Biotechnol 2007;82(4):382–8.
[17] Carbonell AM, Kercher KW, Sing RF, Heniford BT. Susceptibility of prosthetic biomaterials to infection. Surg Endosc 2005;19(12):1670.
[18] Petersen S, Henke G, Freitag M, Faulhaber A, Ludwig K. Deep prosthesis infection in incisional hernia repair: predictive factors and clinical outcome. Eur J Surg 2001;167(6):453–7.
[19] Cobb WS, Paton BL, Novitsky YW, Rosen MJ, Kercher KW, Kuwada TS, et al. Intra-abdominal placement of antimicrobial-impregnated mesh is associated with noninfectious fever. Am Surg 2006;72(12):1205–8. Discussion 1208–1209.
[20] Murray CK, Hsu JR, Solomkin JS, Keeling JJ, Andersen RC, Ficke JR, et al. Prevention and management of infections associated with combat-related extremity injuries. J Trauma 2008;64(Suppl. 3):S239–251.
[21] Campbell AA, Song L, Li XS, Nelson BJ, Bottoni C, Brooks DE, et al. Development, characterization, and anti-microbial efficacy of hydroxyapatite–chlorhexidine coatings produced by surface-induced mineralization. J Biomed Mater Res 2000;53(4):400–7.
[22] Darouiche RO, Mansouri MD, Zakarevicz D, Alsharif A, Landon GC. In vivo efficacy of antimicrobial-coated devices. J Bone Jt Surg Am 2007;89(4):792–7.
[23] Mahan J, Seligson D, Henry SL, Hynes P, Dobbins J. Factors in pin tract infections. Orthopedics 1991;14(3):305–8.
[24] Camuso MR. Far-forward fracture stabilization: external fixation versus splinting. J Am Acad Orthop Surg 2006;14(Spec No. 10):S118–23.
[25] Reddy T, Kano A, Maruyama A, Hadano M, Takahara A. Thermosensitive transparent semi-interpenetrating polymer networks for wound dressing and cell adhesion control. Biomacromolecules 2008;9(4):1313–21.
[26] Cesteros L, Ramirez C, Pecina A, Katime I. Poly(ethylene glycol-beta-cyclodextrin) gels: synthesis and properties. J Appl Polym Sci 2006;102(2):1162–6.
[27] Sekkar V, Gopalakrishnan S, Devi K. Studies on allophanate–urethane networks based on hydroxyl terminated polybutadiene: effect of isocyanate type on the network characteristics. Eur Polym J 2003;39(6):1281–90.
[28] Crow F, Duholke W, Farley K, Hadden C, Hahn D, Kaluzny B, et al. Complete spectroscopic structural characterization of novobiocin, isonovobiocin, decarbamylnovobiocin, 2″-(O-carbamyl)novobiocin, and novobiocin-2″,3″-carbonate. J Heterocyclic Chem 1999;36(2):365–70.
[29] Zhao S, Zhang L, Ma D, Yang C, Yan L. Fabrication of novel supramolecular hydrogels with high mechanical strength and adjustable thermosensitivity. J Phys Chem B 2006;110(33):16503–7.
[30] Banwell E, Abelardo E, Adams D, Birchall M, Corrigan A, Donald A, et al. Rational design and application of responsive alpha-helical peptide hydrogels. Natmater 2009;8(7):596–600.
[31] Ono T, Sugimoto T, Shinkai S, Sada K. Molecular design of superabsorbent polymers for organic solvents by crosslinked lipophilic polyelectrolytes. Adv Funct Mater 2008;18(24):3936–40.
[32] Ono T, Sugimoto T, Shinkai S, Sada K. Lipophilic polyelectrolyte gels as superabsorbent polymers for nonpolar organic solvents. Natmater 2007;6(6):429–33.
[33] Reddy T, Takahara A. Simultaneous and sequential micro-porous semi-interpenetrating polymer network hydrogel films for drug delivery and wound dressing applications. Polymer 2009;50(15):3537–46.
[34] Vanderhooft J, Alcoutlabi M, Magda J, Prestwich G. Rheological properties of cross-linked hyaluronan-gelatin hydrogels for tissue engineering. Macromol Biosci 2009;9(1):20–8.
[35] Daoud-Mahammed S, Grossiord J, Bergua T, Amiel C, Couvreur P, Gref R. Self-assembling cyclodextrin based hydrogels for the sustained delivery of hydrophobic drugs. J Biomed Mater Res A 2008;86A(3):736–48.
[36] Daoud-Mahammed S, Couvreur P, Bouchemal K, Cheron M, Lebas G, Amiel C, et al. Cyclodextrin and polysaccharide-based nanogels: entrapment of two hydrophobic molecules, benzophenone and tamoxifen. Biomacromolecules 2009;10(3):547–54.
[37] Rajewski R, Stella V. Pharmaceutical applications of cyclodextrins.2. In vivo drug delivery. J Pharm Sci 1996;85(11):1142–69.
[38] Loftsson T, Brewster M. Pharmaceutical applications of cyclodextrins.1. Drug solubilization and stabilization. J Pharm Sci 1996;85(10):1017–25.